UPPSALA
UNIVERSITET

Digital Comprehensive Summaries of Uppsala Dissertations from the Faculty of Pharmacy 1

Engineering of Native Cellulose Structure for Pharmaceutical Applications

Influence of Cellulose Crystallinity Index, Surface Area and Pore Volume on Sorption Phenomena

BY
ALBERT MIHRANYAN

ACTA
UNIVERSITATIS
UPSALIENSIS
UPPSALA
2005

ISSN 1651-6192
ISBN 91-554-6130-1
urn:nbn:se:uu:diva-4752

Dissertation presented at Uppsala University to be publicly examined in B41, Biomedical Center, Uppsala, Friday, February 11, 2005 at 09:15 for the degree of Doctor of Philosophy (Faculty of Pharmacy). The examination will be conducted in English.

Abstract
Mihranyan, A. 2005. Engineering of Native Cellulose Structure for Pharmaceutical Applications. Influence of Cellulose Crystallinity Index, Surface Area and Pore Volume on Sorption Phenomena. Acta Universitatis Upsaliensis. *Digital Comprehensive Summaries of Uppsala Dissertations from the Faculty of Pharmacy* 1. 56 pp. Uppsala. ISBN 91-554-6130-1

Cellulose powders from various sources were manufactured and characterized to investigate the influence of their crystallinity index, surface area, and pore volume on sorption phenomena and the relevant pharmaceutical functionality. The influence of the cellulose crystallinity index on moisture sorption was important at low and intermediate relative humidities. At high relative humidities, properties such as surface area and pore volume took precedence in governing the moisture sorption process.

The theory of physical adsorption of gases onto fractal surfaces was useful for understanding the distribution of water in cellulose and the inner nanoscale structure of cellulose particles. It was found that, as a consequence of swelling, moisture induces a fractal nanopore network in cellulose powders that have a low or intermediate degree of crystallinity. On the other hand, no swelling occurs in highly crystalline cellulose powders and moisture sorption is restricted to the walls of the open pores.

No correlation was found between the cellulose crystallinity index and the incorporation and release of nicotine in cellulose mixtures. By loading nicotine in highly porous matrices of the Cladophora sp. algae cellulose, higher stability against oxidative degradation, higher loading capacity, and more steady release into an air-stream was achieved than when commercially available microcrystalline cellulose was loaded.

It was also shown that, by manipulating the structure of cellulose, the undesired hydrolysis of acetylsalicylic acid in mixtures with cellulose can be avoided. It was suggested that a broad hysteresis loop between the moisture adsorption and desorption curves of isotherms at low relative humidities could be indicative of an improved compatibility between acetylsalicylic acid and cellulose.

In all, this thesis demonstrates how the pharmaceutical functionality of microcrystalline cellulose can be improved via engineering of the structure of native cellulose powders.

Keywords: microcrystalline cellulose, Cladophora sp. algae, crystallinity index, surface area and pore volume, fractals, stability

Albert Mihranyan, Department of Pharmacy, Box 580, Uppsala University, SE-75123 Uppsala, Sweden

ISSN 1651-6192
ISBN 91-554-6130-1
urn:nbn:se:uu:diva-4752 (http://urn.kb.se/resolve?urn=urn:nbn:se:uu:diva-4752)

To my mother

“To know wisdom and instruction;
to perceive the words of understanding”

Proverbs 1:2

(also the first words written using the Armenian script)

Papers discussed

The following papers are included in the thesis and will be referred to by their Roman numerals in the text:

I Mihranyan, A., Piñas Llagostera, A., Karmhag, R., Strømme, M., Ek, R. (2004). "Moisture sorption by cellulose powders of varying crystallinity." Int J Pharm 269(2): 433-442.

II Strømme, M., Mihranyan, A., Ek, R., Niklasson, G.A. (2003). "Fractal dimension of cellulose powders analyzed by multilayer BET adsorption of water and nitrogen." J Phys Chem B 107(51): 14378-14382.

III Mihranyan, A., Strømme, M. (2004). "Capillary condensation of moisture in fractal pores of native cellulose powders." Chem Phys Letters 393: 389-392.

IV Mihranyan, A., Andersson, S. B., Ek, R. (2004). "Sorption of nicotine to cellulose powders." Eur J Pharm Sci 22(4): 279-286.

V Mihranyan, A., Strømme, M., Ek, R. "Stability of acetylsalicylic acid in cellulose powders." In manuscript.

Also published:

Strømme, M., Mihranyan, A., Ek, R. (2002) "What to do with all these algae?" Materials Letters 57: 569-572.

A.M. is also a co-author of two patent applications (pending).

Contents

Glossary

AMC	Agglomerated micronized cellulose
A_s	Area of the pore walls covered at pressure *p*
ASA	Acetylsalicylic acid
c	Constant in the gas adsorption models
CrI	Crystallinity index
D	Hausdorff or fractal dimension
D_{cc}	Fractal dimension obtained with fractal capillary condensation
DCPD	Dicalcium phosphate dihydrate
D_{mfBET}	Fractal dimension obtained with multilayer fractal BET analysis
DLP	Diameter of the largest pore
DP	Degree of polymerisation
E_1	Energy of adsorption in the first layer
E_L	Energy of liquefaction in upper layers
$f_n(x)$	BET function for a limited number of layers
I_{002}	Overall intensity of the peak at a 2θ about 22°
I_{am}	Intensity of the baseline at a 2θ about 18°
K(D)	Constant related to a fractal dimension
L	Length scale
LCC	Low crystallinity cellulose
M	Measured quantity
MCC	Microcrystalline cellulose
N	Total number of adsorbed molecules
n	Number of layers
N_m	Number of molecules in monolayer
n_{max}	Number of adsorbed layers corresponding to the cut-off region
p	Partial pressure
PVP	Polyvinylpirrolydone
R	Universal gas constant
RH	Relative humidity
r_h	Mean hydraulic radius
r_p	Mean pore radius
r_k	Pore radius from the Kelvin equation
SEM	Scanning electron microscopy
T	Temperature
T_g	Glass transition temperature
T_{in}	Inlet temperature in the spray-dryer

T_{out}	Outlet temperature in the spray dryer
V	Total volume of gas adsorbed
V_m	Volume of gas in a monolayer
V_{mol}	Molar volume
V_p	Volume of gas at a given pressure *p*
x	Relative pressure
x_{ads}	Relative pressure at which pores are filled
x_{des}	Relative pressure at which pores are emptied
XRD	X-ray diffraction
γ	Surface tension
λ	Wave-length
ν	Constant in the FHH model
ζ	Cut-off region

Introduction

Background

Microcrystalline cellulose (MCC) is a purified, partly depolymerized cellulose prepared by treating α-cellulose, obtained as a pulp from fibrous plant material, with mineral acid (European Pharmacopoeia, 2002). MCC occupies an important niche among tabletting excipients because of its excellent properties in direct compression. It is also used for preparation of pellets via wet granulation and as a suspending agent in cosmetics and food products.

Cellulose structure

In 1838, Anselme Payen, a French chemist and industrialist, discovered a substance later recognized as the most abundant polymer on Earth: cellulose (Payen, 1838). The cellulose obtained from nature is referred to as cellulose I (or native cellulose). There are, however, other modifications of cellulose, namely cellulose II, III, and IV, produced by special treatment of native cellulose (Marchessault and Sarko, 1967; Walton and Blackwell, 1973; Marchessault and Sundararajan, 1983).

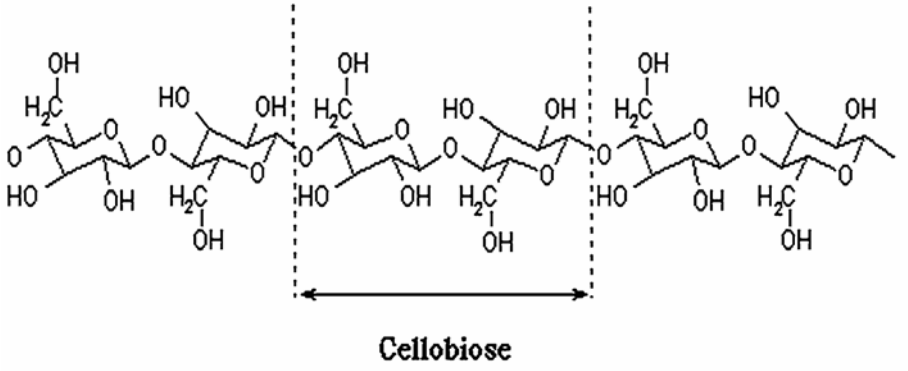

Figure 1. Schematic view of an extended cellulose chain.

Native cellulose is a mixture of two allomorphs: cellulose Iα and Iβ (vander Hart and Atalla, 1984). The triclinic Iα allomorph is predominant in algal-bacterial celluloses, whereas the cotton-ramie types of cellulose are rich in the monoclinic Iβ form (Horii et al., 1987).

The principal monomer of cellulose is β-1, 4-linked D-glucopyranose. The adjacent monomer units are arranged so that glucosidic oxygens point in opposite directions to form a so-called cellobiose unit, Figure 1. These cellobiose units are linked to form an extended, straight chain. The length of the cellulose chain is denoted as the degree of polymerisation (DP) which, in nature, approximates 10,000-15,000 glucopyranose units (Sjöström, 1981). During the manufacture of MCC, the chain length is significantly reduced to a DP of about 100-200 units (Doelker et al., 1987).

The key for understanding the macromolecular structure of cellulose is the arrangement of the glucose molecule itself (Ståhlberg, 1991). Glucose is most stable in the "chair" conformation of its pyranose rings from where all of its hydroxyl groups are in equatorial position. Around the circumference of the ring, it has a polar character, whereas the "top" and "bottom" planes are more hydrophobic. Consequently, the β-1, 4-linked straight chains in native cellulose have hydrophilic edges and hydrophobic core. This offers good opportunities for hydrogen bonding in one direction and for hydrophobic and van der Waals interactions in the perpendicular direction. As a result, the chains are capable of forming highly crystalline microfibrils with a hydrophobic interior. This structure makes cellulose highly inert and resistant to chemical reagents. It could also explain why oligomers with a DP of 6 or higher are practically insoluble, despite the good solubility of both glucose and cellobiose.

Cellulose crystallinity

All celluloses contain a portion of chains that lack order, often referred to as "amorphous" cellulose. The crystalline fraction is generally expressed in percent as the crystallinity index. Various methods of assessing the crystallinity index are available, namely X-ray diffraction (Segal et al., 1959), CP/MAS ^{13}C solid-state NMR (vander Hart and Atalla, 1984), and Fourier transform IR-spectroscopy (Nelson and O'Connor, 1964). However, the absolute values of the crystallinity index vary with the method used and it is thus important that the evaluation procedure is specified.

The crystallinity index of native cellulose powders may be lowered either by grinding (Nakai et al., 1977; Suzuki and Nakagami, 1999) or by addition of

swelling agents (Patil et al., 1965). In contrast, extraction of cellulose from the cell walls of certain algae produces highly crystalline cellulose (Ek et al., 1998).

Cellulose from *Valonia ventricosa* algae (especially acid-hydrolysed *Valonia* or microcrystalline *Valonia*) has the highest crystallinity among the available cellulose types and is considered to be the reference in this respect (O'Sullivan, 1997). The crystalline domains in *Valonia* are individual microfibrils. Of the 600-1000 parallel chains that may exist in a *Valonia* microfibril, only 6-7% are "amorphous". In fact, Verlhac et al. (1990) suggested that the areas that appear "amorphous" are mainly composed of surface chains. This argument is in agreement with the findings of other authors for cellulose from the Cladophora sp. algae (Wickholm et al., 1998; Gustafsson et al., 2003).

Whilst X-ray diffraction analysis and other methods undoubtedly indicate various degrees of order in MCC, parameters, such as Tg, which are directly associated with the amorphous state, cannot be reliably reproduced (Stubberud et al., 1996).

This all implies that, unlike materials which have low molecular weights and lack the fibrillar structure associated with strong intermolecular bonding, cellulose cannot be described by the term "amorphous" in its original meaning (i.e. "liquid-like").

Swelling of cellulose

The swelling in native cellulose can occur either between crystallites, i.e. *intercrystalline* swelling, or within crystallites, i.e. *intracrystalline* swelling, (Sjöström, 1981). Intracrystalline swelling can be achieved using concentrated solutions of alkali, strong acids, or certain salts. This type of swelling can be either *limited* (without complete destruction of the interchain bonding) or *unlimited* (resulting in complete dissolution of the cellulose).

Surface area and pore structure

The surface area of a solid may be defined as the total area that this material exposes to its environment (Alderborn and Nyström, 1993). It is often useful to distinguish between *external* and *internal* surface areas. One convention is to define the external surface area as including all prominences plus the sur-

face of all those cracks that are wider than they are deep (Sing et al., 1985). The internal surface area then comprises the walls of cracks, pores and cavities that are deeper than they are wide while remaining accessible to the analyzing medium.

Methods designed to assess the surface area commonly utilize interactions between a solid and another phase or a light beam (Rouquerol et al., 1994). However, the results depend on the method used and the capacity of the analyzing medium to penetrate the pore structure. In this context, it is expedient to classify pores according to their size and accessibility (Sing et al., 1985). For example, when classifying according to accessibility, an *open pore* is a cavity or channel communicating with the surface of the particle, as opposed to a *closed pore*. A *void* is the space or interstice between particles. When classifying according to size, pores can be defined as *macropores* (pore diameter > 50 nm), *mesopores* (pore diameter between 2 nm and 50 nm), and *micropores* (pore diameter < 2 nm).

Adsorption isotherms

When a gas is brought into contact with a solid, some of the gas molecules will become attached to the surface of the solid to reduce the free energy of the system. At each given relative pressure x, the thickness of the adsorbed layer is not uniform but rather represents a statistical distribution of patches of molecules attached to the surface (Hill, 1946), Figure 2.

However, application of advanced statistical mechanics to physical adsorption requires elaborate mathematics and is not practically expedient. Therefore, in spite of utilizing rather crude assumptions, the BET theory of multimolecular gas adsorption remains the basis for the most widely used method of estimating surface areas.

BET and GAB equations

The BET method (Brunauer et al., 1938) was designed for flat homogeneous surfaces where adsorbed molecules in one layer act as adsorption sites in consecutive layers. By assuming that the energy of adsorption in the second and all higher layers equals the energy of liquefaction of the adsorptive gas, and that the multilayer has infinite thickness at relative pressure x = 1, the following equation was derived:

$$\frac{V}{V_m} = \frac{cx}{(1-x)(1-x+cx)} \qquad (1)$$

where $c = k \exp(E_1 - E_L) / RT$ (2)

The BET method fits experimental data very well at low relative pressures (x ≤ 0.35-0.40). An extension of the BET method, which included the concept of an intermediate state of vapor between the first layer and condensed upper layers enabled Guggenheim, Anderson and de Boer to independently derive a formula (the GAB equation) that produces better fits at high relative pressures x (Anderson, 1946; Guggenheim, 1966; de Boer, 1968).

Figure 2. Adsorption of gas molecules onto solid surfaces.

FHH equation

Because there will be a gradual shift to more liquid-like properties as the number of adsorbed layers increases, Frenkel, Halsey and Hill (Hill, 1952) assumed that the adsorbed layer forms a liquid film on the surface of the adsorbent. As a result, the following isotherm equation was derived for large V/V_m

$$\frac{V}{V_m} \propto \left(RT \ln \frac{1}{x} \right)^{-\nu} \quad (3)$$

where the exponent ν is a parameter characterizing the shape of the isotherm in the multilayer region.

Kelvin equation and hysteresis

Adsorption analysis can also be used to derive information about the pore structure of a material (Rouquerol et al., 1994). The total pore volume, V_p, is often obtained from the amount of gas adsorbed at a relative pressure close to unity by assuming that all pores are then filled with the condensed adsorptive in its normal liquid state. This process is referred to as *capillary condensation* (Sing et al., 1985).

The mean hydraulic radius of a group of mesopores is defined as

$$r_h = (\frac{V}{A_s})_p \quad (4)$$

where $(V/A_s)_p$ is the ratio of the volume to the surface area of the pore walls for the group. For non-intersecting cylindrical capillaries the relationship between the mean hydraulic radius, r_h, and mean pore radius, r_p, is

$$r_p = 2r_h \quad (5)$$

The Kelvin equation is generally used to obtain the pore size distribution from capillary condensation in mesoporous materials (Kelvin, 1871)

$$r_k = -\frac{2\gamma V_{mol}}{RT \ln x} \quad (6)$$

where γ is the surface tension of the liquid condensate and V_{mol} is the molar volume.

Physisorption in porous materials is often accompanied by hysteresis arising between the adsorption and desorption curves of isotherms. This may be due to differences in condensation and evaporation occurring in pores of varying geometry (e.g. "ink bottle" pore). However, hysteresis loops are also known to arise in cylindrical pores. According to Cohan (1938), this is due to differences in the menisci during adsorption and desorption caused by the fact that pores are filled radially during adsorption but emptied axially during desorption, Figure 3.

Figure 3. Origin of hysteresis between adsorption (left) and desorption (right) curves.

Thus, for cylindrical pores, the following relationship will hold

$$x_{ads}^2 = x_{des} \quad (7)$$

where x_{ads} is the relative pressure at which the pore is filled and x_{des} is the relative pressure at which the pore is emptied. It should be mentioned that this simple rule holds for $x \geq 0.35\text{-}0.40$ (Pomonis and Ladavos, 2002). However, in some cases a hysteresis loop is also observed in a region of lower pressure ($x \leq 0.35\text{-}0.40$). This phenomenon may be associated with swelling or some other kind of interaction between the sorbent and sorptive (Sing et al., 1985).

The concept of fractals

Although key concepts associated with fractal geometry had been separately studied for years by mathematicians (e.g. Hausdorff, Koch, Julia, etc), Mandelbrot was the first to point out that fractals were an ideal tool for modeling a variety of natural phenomena (Mandelbrot, 1982). According to Mandelbrot, the general description of non-uniform phenomena is as follows

$$M \propto L^D \tag{8}$$

where M is the measured quantity, L is the length scale, and D is the fractal dimension (non-integer). The impact of this simple formula on our understanding of such elementary geometrical concepts as surface area or porosity is tremendous. Another remarkable property of fractal geometry is its applicability to disordered media based on the observation that many disordered systems possess *scale symmetry*. In the field of pharmaceutics, the concept of fractals together with the percolation theory have been successfully applied to model tablet compaction and drug release phenomena (Leuenberger et al., 1996).

What is a fractal surface?

In classical Euclidean geometry, the surface area of a planar object is described by two dimensions (length and breadth). However, surfaces in nature are rarely planar and are sometimes so irregular that a traditional, two-dimensional perception of the surface ceases to be meaningful. For instance, how could one define the surface of an extremely porous or amorphous sorbent? Indeed, in an extreme case a surface may fold back and forth in such a manner that monolayer formation amounts to penetration of the sorptive into virtually the entire solid. Then, if one ignores the thin walls of the supporting adsorbent material or considers the latter as a “solvent” (as is the case with amorphous solids), the molecules end up in an arrangement that resembles

three-dimensional bulk rather than a two-dimensional sheet. Obviously, these irregularities of the surface can no longer be treated as mere deviations from the surface planarity but rather as an intrinsic property of the surface with dimensions somewhere between 2 and 3 (Pfeifer and Avnir, 1983).

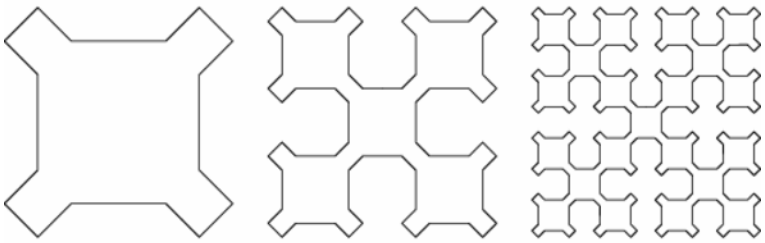

Figure 4. Sierpinski curve.

Some systems are called *exact fractals* because their self-similarity is exact at every length scale, Figure 4. However, many systems, especially those in nature, are self-similar only in a *statistical* or *average* sense. A solid particle can have a fractal surface in three ways. If it is a *surface fractal*, only the surface is folded fractally. If it is a *mass fractal*, both the surface and bulk exhibit fractal behavior. In a *pore fractal*, both the surface and pore space are fractals. Pore fractals are very rare (only one example has been reported to date (Pfeifer et al., 2002)) and the most materials exhibiting fractal behavior have been described either as mass fractals or as surface fractals. Surface fractals comprise the largest and most diverse group of fractal objects in nature (Avnir et al., 1992). Mass fractals are usually aggregates, i.e. loosely bound structures of low mechanical strength whose density drops as the size of the object is increased. However, mass fractals with high mechanical strength have also been reported (Brady and Ball, 1984; Schaefer and Keefer, 1986). Pfeifer et al. (1989a) demonstrated that fractal BET analysis is appropriate for mass fractals, whereas fractal FHH analysis better suits surface fractals.

Fractal analysis of adsorption isotherms

Until recently, the bulk of surface science models concentrated on the thermodynamics of sorption and little attention was given to geometry, mainly because of the complexity involved (Avnir et al., 1992). Fractal analysis of adsorption isotherms was first introduced by Avnir and Pfeifer (1983) and has since become a powerful tool in an exceedingly diverse list of molecular-surface phenomena. The multilayer fractal BET (mfBET) analysis, de-

veloped by Pfeifer et al. (1989b), is a generalization of the work by Brunauer, Emmet, and Teller and gives the number of adsorbed molecules N as

$$\frac{N}{N_m} = \frac{(D-1)}{(1-n_{\max}^{1-D})} \int_1^{n_{\max}} n^{1-D} f_n(x) dn \tag{9}$$

where

$$f_n(x) = \frac{cx}{(1-x)} \frac{1-(n+1)x^n + nx^{n+1}}{1+(c-1)x - cx^{n+1}} \tag{10}$$

In the equation 9, D is the fractal dimension of the distribution of sites at which the molecules are adsorbed and N_m is a parameter related to the monolayer capacity. In the non-fractal case ($D=2$), N_m equals the number of molecules in the monolayer. Further, n_{max} represents the number of adsorbed layers corresponding to the cut-off of the fractal region. The adsorption strength is denoted by c, as in the classical BET model. It should be noted that this version of mfBET assumes that the dimension of the embedding space of the material under investigation is 3 and that the topological dimension is 1, which is true for almost all mass fractals.

In fractal FHH theory, the relationship including the effects of surface tension is as follows (Pfeifer et al., 1989a)

$$\frac{N}{N_m} \propto K(D) \left(\ln \frac{1}{x} \right)^{-(3-D)} \tag{11}$$

Interestingly, Avnir and Jaroniec (1989) have also derived this equation for the Dubinin-Radushkevich model typically used for micropore filling. The combination of the FHH equation with the Kelvin equation yielded a formula that accounts for capillary condensation in fractal pores (Yin, 1991):

$$\frac{N}{N_m} \propto \frac{D-2}{3-D} \left(\ln \frac{1}{x} \right)^{-(3-D)} \tag{12}$$

It should be mentioned that the fractal capillary condensation theory is applicable only for surface fractals. Furthermore, contrary to the multilayer models where adsorption occurs layer by layer, the adsorption process in the fractal capillary condensation theory assumes sequential filling of pores of increasing radii.

Surface area of native cellulose

For MCC, a specific surface area of around 1 m^2/g measured with BET N_2 gas adsorption has been reported (Handbook of Pharmaceutical Excipients, 1994). On the other hand, applying the BET method to water sorption isotherms yields surface area values of around 130-150 m^2/g (Nakai et al., 1977; Hollenbeck et al., 1978). Zografi et al. (1984) elucidated the differences between N_2 and H_2O BET analysis, which will be discussed in detail below.

Moisture sorption by native cellulose

For polymers that give well-defined X-ray crystalline diagrams, the question is whether or not water penetrates the crystallites. Moisture sorption does occur in the crystallites of certain polymers, e.g. alginic acid (Astbury, 1945) or proteins such as collagen and gelatin (Bear, 1944). However, as a rule of thumb, the crystallites of polymers that can form fibers with strong intermolecular bonding remain inaccessible to water (Valentine, 1958).

It was found that moisture does not penetrate the crystallites of cellulose, but it is sorbed in the disordered regions located in the bulk of particles (Howsman, 1949). Zografi and Kontny (1986) argued that, since moisture uptake occurs in the "amorphous" bulk of the particles, the apparent surface area values obtained with H_2O BET are physically meaningless. In an attempt to elucidate the mechanisms of water/cellulose interactions, Zografi et al. (1984) proposed that interactions between water and cellulose occur in three stages and that three states of water can exist in cellulose. At low and intermediate RHs, water molecules primarily bind to the anhydroglucose units of cellulose chains with different stoichiometry, corresponding to stages one and two, respectively. However, at RHs above 60%, water molecules can also bind to other water molecules which are not attached to the primary sites, thus acquiring properties of bulk liquid. Later calorimetric studies supported this three-stage model (Blair et al., 1990).

Is sorption in the bulk of solid necessarily absorption?

In the Zografi model of water sorption by MCC, the water uptake is considered to be essentially an *absorption* process. Absorption, which (except for the cases of wave and/or energy absorption) refers to uptake of substances by liquids or amorphous solids, fundamentally resembles dissolution. In the

case of moisture absorption by amorphous solids, the solid is the solvent (i.e. excess phase) and water is the solute. Several solution-based models have been derived to describe the absorption into amorphous solids, e.g. Flory-Huggins (Flory, 1953), Hailwood-Horrobin (Hailwood and Horrobin, 1946), and Vrentas-Vrentas (Vrentas and Vrentas, 1994a, 1994b) models. Indeed, at least for sugars and low molecular weight polymers such as PVP, solution-based models were found valid (Hancock and Zografi, 1993; Zhang and Zografi, 2000).

It should however be borne in mind that dissolution results in single-phase systems where the solute molecules are more or less homogeneously dispersed throughout the excess of the solvent. The three-stage model of moisture sorption by cellulose does not fit with the assumption of absorption-dissolution because of the presence of two phases, i.e. clusters of bulk water restricted within the excess of the solid phase (cellulose). Another remarkable shortcoming of solution-based models is their failure to predict the hysteresis. Hence, the question of how moisture is accommodated in the bulk of cellulose, with respect to its supra-molecular order, remains open and was one of the objectives of this thesis.

Liquid drug sorption

A number of drug compounds, such as nicotine, nitroglycerine or valproic acid, are liquids. Depending on the carrier's structure, loading of liquid drugs could be accomplished differently, Figure 5:

- the liquid could be distributed in the voids between individual carrier particles (granulation),
- it could be loaded in the internal pores of individual carrier particles, or
- if the carrier material is amorphous, it could be incorporated inside the bulk of individual particles.

The release of the drug from the carrier, as well as the stability of the drug, can be influenced by the method used in preparing the drug/carrier system.

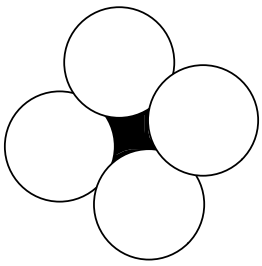

Type I

Type II

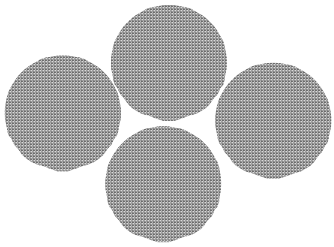

Type III

Figure 5. Schematic drawings of the possible distribution patterns of a liquid compound on a solid carrier. Type I. The liquid compound is distributed in the external porous system (voids between particles). Type II. The liquid compound is distributed in the internal pores of the carrier particles. Type III. The liquid compound is distributed in the disordered regions in the bulk of the carrier particles.

Nicotine formulation aspects

Nicotine products used as smoking substitutes and/or smoking cessation aids can contain nicotine in different forms, e.g. free base nicotine, a nicotine salt, a nicotine complex containing an ion exchanger, or a nicotine inclusion complex. The most effective way of administering nicotine is in its free base form, because it is this form that readily penetrates membranes (Svensson, 1987; Russel, 1988). However, free base nicotine is a labile compound that is easily lost by evaporation and/or oxidative degradation (Jackson, 1941).

Interestingly, the stability of liquid compounds has been successfully addressed in the field of explosive materials. For example, nitroglycerin was stabilized against detonation to produce dynamite (Encyclopaedia Britannica, 2003). The basis for the discovery was a highly porous material, kieselguhr, capable of adsorbing large quantities of nitroglycerin to produce an essentially dry granular powder. Later wood pulp was substituted for kieselguhr as the adsorbent.

Reactions in the solid-state

Chemical reactions occur as a result of collisions between molecules, according to definite statistical laws. If the reactants are distributed homogeneously on an atomic or molecular level (e.g. true solutions or gases), the system can be described by equations involving only time and concentration. However, reactions in the solid state occur almost exclusively at interfaces. The difficulty lies, therefore, not only in defining the reacting concentrations at the interface but also in accounting for the presence of the so-called “hot-spots” of higher local reactivity and the diffusion of the reactants and/or products to/from the interface. The most common types of solid-state reactions include (Hulbert, 1970; Šeštak et al., 1973):

- Chemical order reactions,
- Nucleation-and-growth controlled reactions,
- Diffusion controlled reactions, and
- Phase-boundary controlled reactions.

ASA formulation aspects in mixtures with cellulose

The solid-state stability of drugs in mixtures with excipients is sometimes different from that of the pure drug. For instance, the degradation of acetylsalicylic acid (ASA) in mixtures with MCC is accelerated compared with the degradation of pure ASA (Ahlneck and Lundgren, 1985). MCC is a material with versatile pharmaceutical functionality, especially in tabletting; therefore, stability aspects of drugs in mixtures with MCC are of great importance. Ordinary MCC is manufactured with 4-5% (w/w) moisture content (Handbook of pharmaceutical excipients, 1994). However, to avoid hydrolysis of moisture-sensitive drugs, low moisture grades of MCC are also manufactured (1.5%, w/w, in Avicel PH 112 and 3%, w/w, in Avicel PH 103, FMC Corp). It should, however, be borne in mind that a critical factor for understanding moisture-induced phenomena in multi-component pharmaceutical systems is the distribution of moisture between the drug and excipients rather than the overall moisture content as such. Knowledge about the distribution of moisture within multi-component pharmaceutical systems and the means of achieving the desired functionality by manipulating this distribution is scarce and extending this knowledge was one of the objectives of this thesis.

Aims of the thesis

The overall aim of this thesis was to investigate the influence of cellulose crystallinity index, surface area, and pore volume on sorption phenomena and relevant processes of pharmaceutical importance. The specific aims were:

- To investigate the role of cellulose crystallinity index, surface area, and pore volume on moisture sorption (Paper I),
- To show that multilayer fractal BET (mfBET) theory could be a useful tool to obtain information about the distribution of water in cellulose powders of varying crystallinity (Paper II),
- To show that capillary condensation theory in fractal pores could reveal additional information about the structure of the bulk of cellulose particles (Paper III),
- To examine the influence of cellulose crystallinity index, surface area and pore volume on nicotine sorption, release and stability (Paper IV),
- To investigate the solid-state stability of acetylsalicylic acid in binary mixtures with cellulose powders (Paper V).

Materials and Methods

Materials

Five different types of cellulose were used: microcrystalline cellulose (MCC), agglomerated micronized cellulose (AMC), low crystallinity cellulose (LCC), Algiflor brown algae cellulose, and Cladophora green algae cellulose.

Microcrystalline cellulose (MCC)

MCC (Avicel PH 102, FMC, Ireland) was used as supplied.

Agglomerated micronized cellulose (AMC)

To 100 g of MCC, 50 ml of water was added and the mixture was ground in a mortar mill (Retsch KM 1, Germany) for 2 hours (Papers I-IV) or 4 hours (Paper V). Water was added to form a 10% (dry solids) suspension, followed by spray drying (Minor Type 53, Niro Atomizer A.S., Denmark) at T_{in}=205–210ºC and T_{out}=95–100ºC and a feed rate of 1.7 l/hr.

Low crystallinity cellulose (LCC)

To produce LCC, 50 g of MCC was immersed in 1 l of 70% (w/w) $ZnCl_2$ solution and vigorously stirred. After being allowed to swell for 1 hour, the cellulose was precipitated with additional water. The resultant product was washed repeatedly until the conductivity of the washed water approximated that of deionized water (i.e. 10^{-6} S/cm), and subsequently spray-dried as described above.

Algae cellulose

The Algiflor brown algae (Algiflor, Danisco, France) were a blend of five species: *Laminaria digitata, Lessonia nigrescens, Macrocystis pyrifera, Ascophyllum nodosum,* and *Fucus serratus*. *Cladophora* sp. green algae were harvested from the Baltic Sea

500 g of algae (green or brown) were bleached with 180 g of $NaClO_2$ in 0.5 l of acetic buffer. The mixture was diluted to 5 l, poured into a plastic bag and stored in a water bath for 3 hours at 60ºC. The algae were washed to neutrality (pH~7), as indicated by the color of a pH paper (Universalindikator, Merck, Sweden), and filtered. 3 l of 0.5 M NaOH was added to the remainder, and the resultant product was stored overnight at 60ºC in a water bath. The resultant pulp was washed to neutrality, filtered, and dried at room temperature. The dry, purified algae were ground in a hammer mill (Fitz Mill type D6, Manesty Machines, UK) prior to acid hydrolysis. To 50 g of dry, purified algae 1 l of 5% HCl was added, and the suspension was heated to boiling. Once boiling, it was removed from the heat and the slurry was allowed to stand overnight. The cellulose was then washed to neutrality again and spray-dried as described above.

Nicotine

Nicotine (Siegfried, Switzerland) was used as supplied.

Acetylsalicylic acid (ASA)

ASA (Sigma Aldrich Chemie Gmbh, Germany) was used as supplied.

Methods

Crystallinity index

An X-ray diffractometer with Bragg-Brentano geometry (Diffraktometer D5000, Siemens, Germany) and CuKα radiation was used (λ=1.54 Å). The crystallinity index was calculated as

$$CrI = \frac{I_{002} - I_{am}}{I_{002}} \quad (13)$$

where I_{002} is the overall intensity of the peak at a 2θ of about 22º and I_{am} is the intensity of the baseline at a 2θ of about 18º (Segal et al., 1959). The crystallite size was calculated using Scherer's formula with the assistance of the TOPAS program.

Specific surface area

The BET (N_2) technique was used to estimate the surface area by a multi-point (5 points) determination (ASAP 2010, Micromeritics, USA). The weight of each sample was chosen so as to produce a total surface area of 5–10 m^2. The surface area available for water adsorption was calculated based on similar principles for RHs below 40%. The total pore volume of the powders was obtained as the volume of adsorbed nitrogen/moisture at relative pressure/humidity approximating unity.

Moisture sorption

The moisture content was measured gravimetrically after samples had been stored at 25ºC over saturated salt solutions of LiCl, CH_3COOK, K_2CO_3, NaBr, NaCl, or KNO_3 corresponding to 11, 25, 40, 63, 75, and 96% RHs, respectively (Nyqvist, 1983) for at least 48 hours. Prior to the measurements, the samples were stored over P_2O_5 (0% RH) for 10 days.

Fractal analysis

The mfBET method was used as described in Pfeifer et al. (1989a). The fractal capillary condensation method was used as described in Yin (1991).

Scanning electron microscopy (SEM)

Micrographs of each sample were taken (Leo Gemini 1550 FEG SEM, UK) at 100 000 times magnification. The samples of each powder were coated with gold under vacuum.

Loading of cellulose with nicotine

Rotary evaporation

Approximately 1 g of carefully weighed cellulose powder was washed with ethanol for 20 min. Loading was performed from a nicotine/ethanol solution (10 ml) in a rotary evaporator (Heidolph WB2000, Germany) with a rotation velocity of 90 rpm, the vacuum set at 200 mbar and at a temperature of 60ºC. Prior to applying the vacuum and heating, the cellulose powder was mixed with the ethanol/nicotine solution for 10 minutes at room temperature and 90 rpm. Various concentrations of nicotine in ethanol were used until the maximum loading was achieved. The resultant products were also judged by visual examination (i.e. no wet granular masses were accepted after evaporation of the ethanol).

In contact with air saturated with nicotine

Approximately 1 g of a carefully weighed sample of cellulose powder was placed in a desiccator with a shallow open vessel containing pure nicotine at the bottom. Exposures to nicotine vapor were performed at 22, 40 and 60ºC for 5 days. The loading was obtained as a weight increase, and the mean for three samples was calculated.

Determination of total nicotine content

About 50 mg of the nicotine-loaded cellulose powder was carefully weighed and transferred to a glass flask. Precisely 50.0 ml of 0.05 M sulfuric acid was added and nicotine was extracted by shaking on a mechanical shaker for 20 min. A portion of an extract was centrifuged, and the clear solution was then diluted with 0.05 M sulfuric acid if necessary. The final solution was measured in a UV spectrophotometer at a wavelength of 259 nm (n=3).

Nicotine release into an air-stream

The amount of nicotine released from the nicotine-loaded cellulose powder into a passing stream of air was measured by allowing the airstream to penetrate through a powder plug before entering a solution consisting of 0.05 M sulfuric acid. The cellulose powder was fixed between two pieces of porous membrane (made of polyester/polyamide microfiber). The released gaseous nicotine was trapped in the diluted solution of sulfuric acid. The air-stream was set at 1.0 l/min, and the release test was conducted at 22ºC. The concen-

tration of nicotine in sulfuric acid was measured using a UV spectrophotometer at a wavelength of 259 nm (n=3).

Nicotine release into water

The amount of nicotine released into water was estimated using a dissolution apparatus according to Ph. Eur. 2.9.3., Paddle method (European Pharmacopoeia, 2002). Precisely 500 ml of deionized water was added to each vessel, and the test was performed at 37ºC. Approximately 50 mg of carefully weighed nicotine-loaded cellulose powder was used in each measurement. The nicotine content in a 3 ml sample was analyzed by adding 60 µl 2.5 M sulfuric acid and measuring the absorbance with an UV spectrophotometer at a wavelength of 259 nm (n=3).

Nicotine stability

Approximately 1 g samples of nicotine-loaded powder (prepared by rotary evaporation) were stored in 145 ml glass jars with Teflon-lined screw caps for 3 months in a climate chamber at 25ºC. A Gynkotek liquid chromatographic system was used for the analyses. A Waters Nova-Pak C18 column and a mobile phase consisting of acetonitrile (250 ml) and aqueous phosphate buffer pH=4.5 with added dodecyl sulfate (750 ml) were used for the separation of nicotine and its degradation products. The compounds were detected using a UV spectrophotometer at a wavelength of 254 nm.

Loading of cellulose with ASA

Rotary evaporation

10 ml of 10% (w/v) ASA in ethanol solution was added to 3 g of cellulose powder samples in a round-bottomed flask. The cellulose was loaded using a rotary evaporator (Büchi, Switzerland) at 60ºC. Prior to applying the vacuum and heating, rotation was applied for 5 minutes to thoroughly mix the cellulose powder with the ethanol solution of ASA at room temperature.

Physical mixture

1 g of ASA was mixed with 3 g of each cellulose powder sample using a Turbula mixer (Willy A. Bachofen AG, Switzerland) for 15 minutes.

Storage of ASA/cellulose mixtures

The loaded cellulose samples were stored at 50ºC in dessicators with saturated solutions of LiCl, K_2CO_3, NaBr, NaCl, or KNO_3 corresponding to RHs of approximately 11, 40, 50, 75, and 90% respectively. The salicylic acid content was measured after loading at different time points during 2 months as described below.

ASA degradation products

The degradation of ASA was examined with a UV-spectrophotometer (Hitachi U1100, Japan) by measuring the absorbance of salicylic acid in 95% ethanol at 303nm (E1% 1 cm at 303 nm= 262) at regular intervals (Ahlneck and Alderborn, 1988). Approximately 50 mg of the ASA-loaded cellulose sample was carefully weighed and 25 ml of 95% ethanol was added. The suspension was vigorously shaken and then centrifuged at 5000 rpm for 5 min (Eppendorf, Germany). The clear solution was pipetted out and subsequently used for the UV analysis.

Results and Discussion

Solid-state characteristics of cellulose powders

Figure 6 shows X-ray diffraction patterns for the cellulose samples. A smeared out diffractogram was observed with LCC indicating low degree of order. The MCC diffractogram revealed a relatively ordered structure, which was only surpassed in order by the Cladophora sample. The cellulose extracted from brown algae was less ordered than that from green algae. The crystallinity indices of the samples and their crystallite sizes as well as the specific surface area values for the cellulose samples are listed in Table 1.

Table 1. *Primary solid-state characteristics of native cellulose powders.*

	Crystallinity index, %	Crystallite size, Å	Specific surface area, m^2/g	
			N_2	H_2O
LCC	45.0	43.7	0.48	204.2
AMC	69.1	45.5	1.13	168.3
MCC	82.2	49.1	0.96	117.3
Algiflor	81.7	41.2	5.76	130.6
Cladophora	95.2	135	94.7	52.80

The crystallite size values for the LCC, AMC, MCC, and Algiflor samples ranged between 41 and 49 Å. However, the crystallite size of the Cladophora cellulose sample was markedly larger. These differences could be traced to the cellulose synthase complexes which determine the size and shape of the cellulose microfibrils (Ståhlberg, 1991). For instance, in all higher plants, the cellulose synthases appear as solitary rosettes of six hexagonally arranged subunits, producing thin microfibrils. In contrast, synthases of certain green algae species, e.g. Valonia, are arranged into large rectangular complexes rather than rosettes, capable of producing extremely thick microfibrils. The specific surface area of Cladophora cellulose powder measured with N_2 BET exceeded the corresponding values of the other samples manifold. The differences between the surface area values obtained with N_2 BET and those for H_2O will be discussed in detail below.

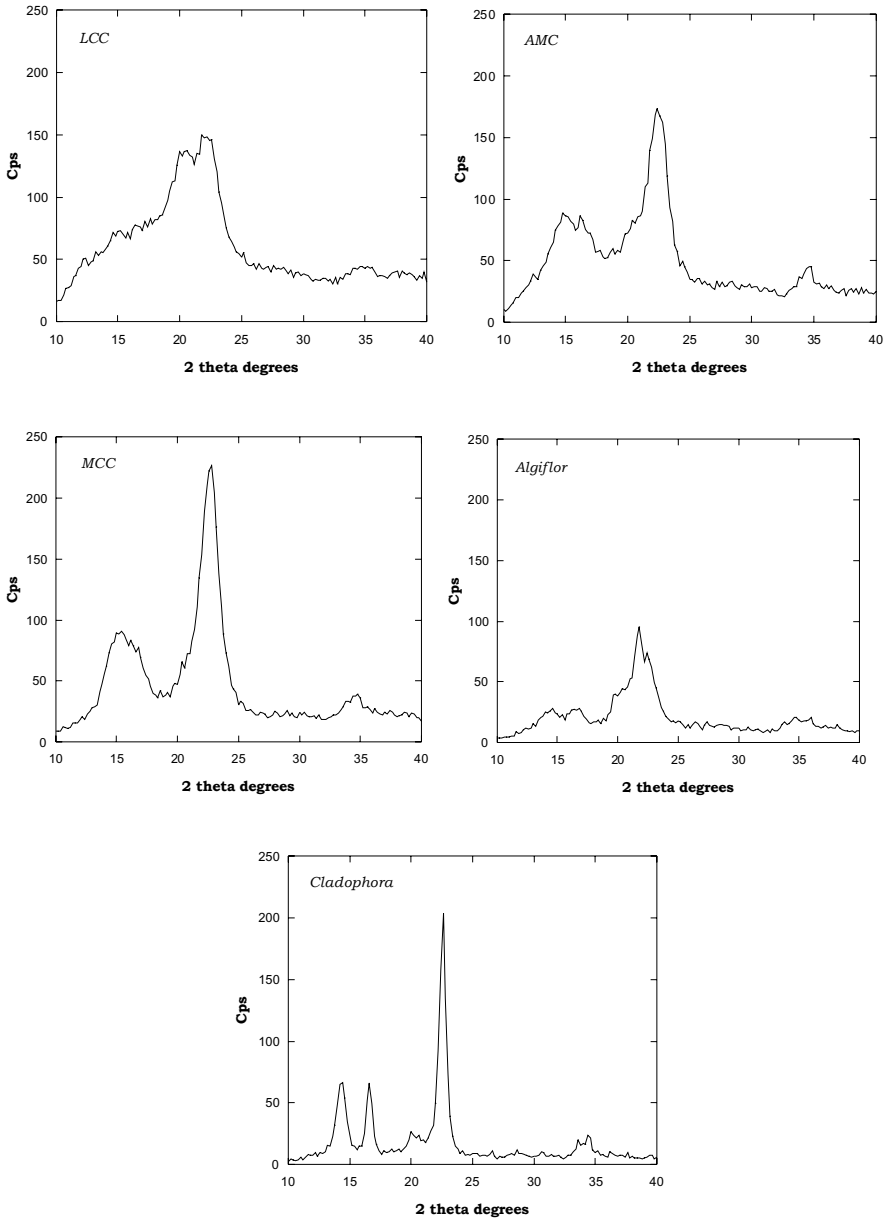

Figure 6. X-ray diffraction patterns for native cellulose powders.

Figure 7 illustrates the texture of the cellulose samples as obtained with SEM. The texture of the Cladophora cellulose sample diverges greatly from that of the rest of the samples, which all have a more or less smooth (although wavy or grooved) structure. The Cladophora cellulose particles had a characteristic web-like structure with distinct filaments. The width of the

filaments, obtained from the SEM micrographs, was around 10-30 nm, which coincides well with the width of the Cladophora microfibril obtained from NMR studies (Wickholm et al., 1998). In contrast to the rest of the samples, the SEM pictures of the Cladophora cellulose particles suggest a very porous structure, which matches the large specific surface area values obtained with N_2 BET adsorption.

LCC AMC

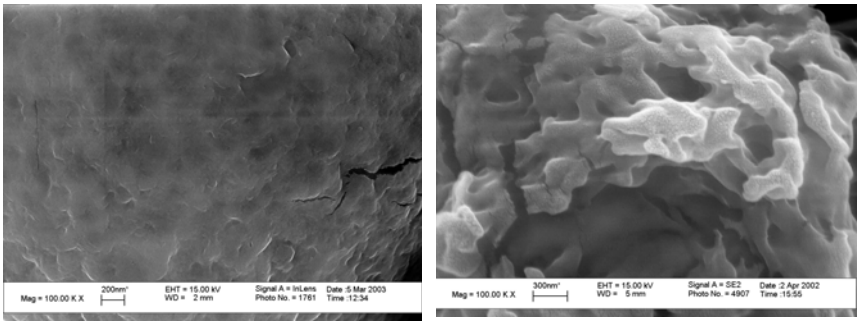

MCC Algiflor

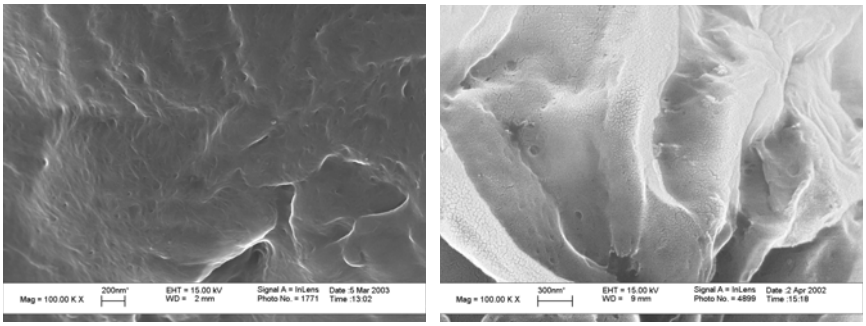

Cladophora

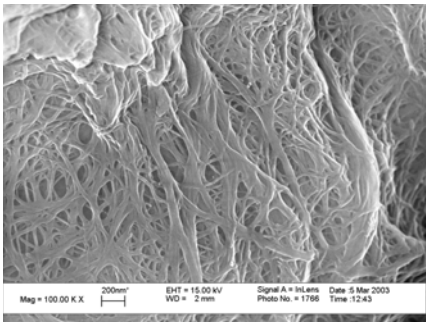

Figure 7. SEM micrographs of native cellulose powders at 100K× magnification.

Moisture sorption by cellulose powders

Moisture sorption isotherms are presented in Figure 8. The moisture sorption was higher for cellulose samples with lower crystallinity index at RHs below 75%. At RHs above 75%, the moisture content of the Cladophora cellulose sample increased sharply. It can be concluded that at very high RHs, the large surface area and pore volume of the cellulose may take precedence over the crystallinity index in governing the moisture sorption pattern. The surface area available for moisture sorption, calculated using the same principles as for N_2 adsorption, was the lowest in the Cladophora sample, whereas the highest values were obtained for LCC, Table 1. It should be mentioned that the surface area and pore volume of the Cladophora cellulose powder were of the same order of magnitude for both N_2 and H_2O BET.

A hysteresis loop was observed between the moisture adsorption and desorption curves for all samples. The level of hysteresis was broader for the cellulose powders with a lower crystallinity index. Hysteresis loops may have different origins for different samples. At high RHs, a loop is often seen in the isotherms of highly porous materials due to capillary condensation, whereas, at low RHs, it is caused by swelling or some other kind of interaction between the sorbent and sorptive. The hysteresis loops seen at low and intermediate RHs in LCC, AMC, MCC and Algiflor samples are likely to be associated with sorption into the bulk of the particles. On the other hand, the hysteresis loop observed in the Cladophora cellulose sample is likely to have arisen as a result of capillary condensation in the porous matrix.

Since moisture cannot penetrate cellulose crystallites, sorption is restricted to the interstitial space between them. When moisture is adsorbed onto the microfibrilar contact surfaces, it causes swelling and this exposes the inner bulk structure of the particles. The ability of moisture to penetrate into the bulk will depend on the number of available OH-groups and, thus, on the crystallinity index. N_2 and other gases, which are commonly used in BET analysis (e.g. Kr or Ar), do not cause swelling, and the surface area available for their sorption is orders of magnitude smaller than that available for moisture. On the other hand, because moisture cannot penetrate into the bulk of highly crystalline Cladophora cellulose particles, the detected surface area available for H_2O and N_2 sorption is of the same order of magnitude.

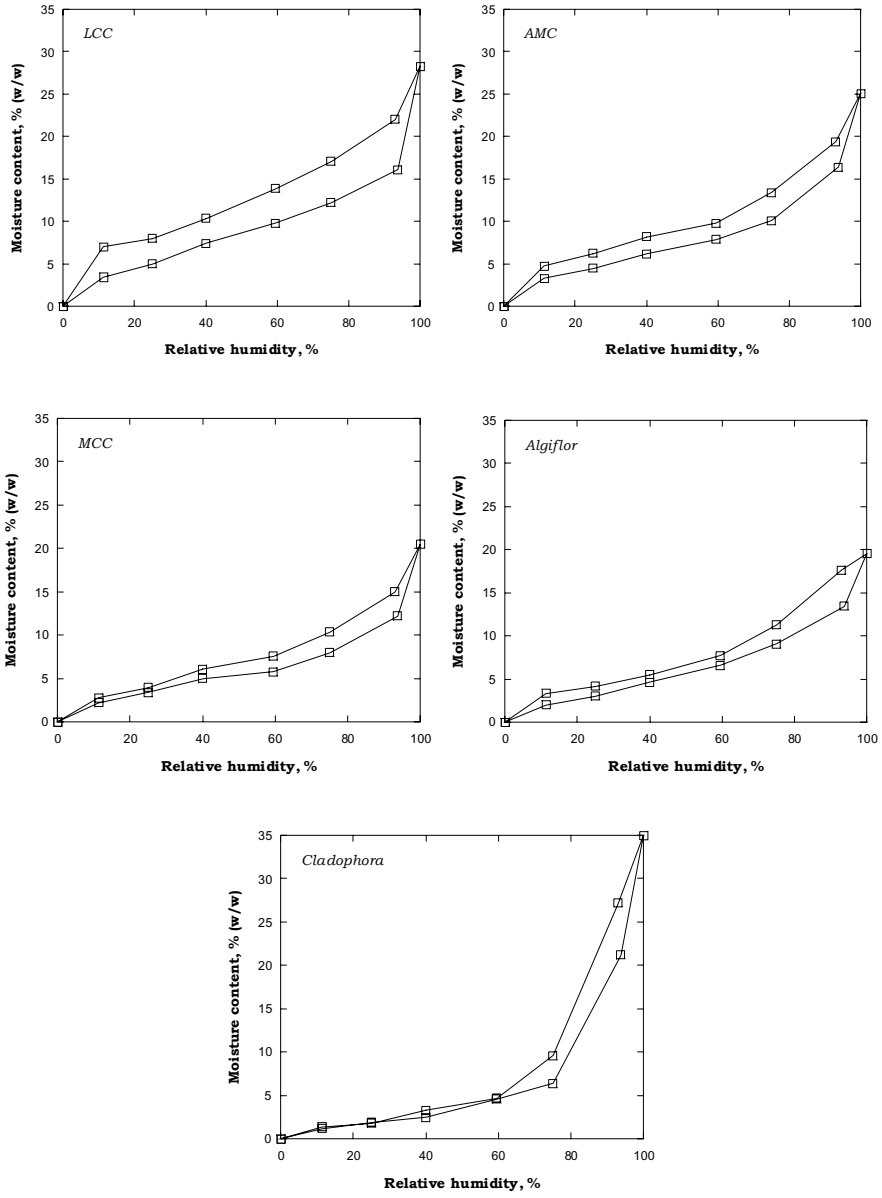

Figure 8. Moisture sorption isotherms of native cellulose powders.

Fractal analysis of water and nitrogen gas adsorption

Fractal analysis was conducted to reveal information about the structure of the bulk of cellulose particles and the distribution of moisture and nitrogen within them. The results for mfBET are summarized in Tables 3 and 4. The characteristic fractal dimension (D_{mfBET}) sensed by N_2 ranged from 2.13 and 2.50, whereas that for H_2O sorption ranged from 1.09 to 1.46. Table 3 shows that, for all the samples except Cladophora cellulose powder, n_{max} was between 12 and 18, which corresponds to a water layer of around 4-5 nm in thickness. The n_{max} value for the Cladophora sample was found equal to 78, which corresponds to a layer thickness of 24 nm. The Cladophora sample was the most crystalline in the series (crystallinity index above 95%). It is therefore likely that the regions available for water sorption in this material are located along the walls of open pores, in contrast to the less ordered samples where water sorption can also take place in the particle bulk. This interpretation is in line with the values for D_{mfBET} in Table 2.

Table 2. *Characteristics of cellulose powders obtained by mfBET analysis of water adsorption isotherms. The values in parentheses are absolute deviations in percent (n=3).*

	Pore volume, cm^3/g	D_{mfBET}	N_m, mg/g	c	n_{max}	Outer cut-off ξ, nm
LCC	0.28 (35)	1.46 (3)	34.4 (8)	10 (21)	12 (16)	3.7
AMC	0.25 (4)	1.39 (2)	19.6 (6)	24 (26)	17 (12)	5.3
MCC	0.20 (11)	1.43 (3)	16.8 (6)	13 (22)	15 (13)	4.7
Algiflor	0.20 (3)	1.32 (2)	19.8 (5)	9.0 (17)	18 (5)	5.6
Cladophora	0.35 (22)	1.09 (2)	11.7 (4)	10 (16)	78 (6)	24

D_{mfBET} is close to unity for the Cladophora sample, which shows that the available regions for sorption of water molecules are not distributed throughout the material but are rather aligned in a quasi-linear array. D_{mfBET} is remarkably higher for other samples, which suggests a more space-filling distribution of activities. This may also explain the relatively large difference in n_{max} between Cladophora and the other materials: water sorption in the bulk of less ordered cellulose particles is confined and requires breakage of polymer-polymer bonds, whereas sorption of water in the Cladophora particles occurs more or less unhindered until the pore space is filled without breakage of polymer-polymer bonds. Thus, the pore size sets an upper limit on the number of layers of water that can be adsorbed. In this context, it is appropriate to mention that, whereas the largest pore diameter sensed by N_2 BET was found to be 98 nm (for the Cladophora sample), the average pore diameter was around 23 nm, which is in close agreement with the water layer thickness of 24 nm probed by H_2O mfBET. The fact that the pore volumes probed by H_2O and N_2 are of the same order of magnitude further sup-

ports the above argument that, in the highly crystalline Cladophora cellulose, water sorption is confined exclusively in the open pore space and no significant swelling occurs. On the other hand, volumes occupied by H_2O for the less ordered cellulose samples are 1-2 orders of magnitude larger than the corresponding volumes for N_2, underlining the importance of swelling. The latter is also supported by earlier NMR studies on MCC (Ek et al., 1995). Hence, the value for the thickness of the water layer obtained using mfBET for the less ordered cellulose samples reflects the extent of swelling between cellulose chains. Table 3 shows that this distance was around 4-5 nm, which is of the same order of magnitude as the width of the microfibrils in wood cellulose.

Table 3. *Characteristics of cellulose powders obtained by mfBET analysis of nitrogen adsorption isotherms. The values in parentheses are absolute deviations in percent (n=3).*

	Pore volume, cm^3/g	DLP, nm	D_{mfBET}	N_m, cm^3 STP /g	c	n_{max}	Outer cut-off ξ, nm
LCC	0.0016 (34)	142 (5)	2.30 (7)	0.022 (10)	189 (21)	910 (11)	304
AMC	0.0044 (23)	137 (3)	2.50 (3)	0.111 (2)	321 (18)	335 (7)	112
MCC	0.0250 (1)	142 (2)	2.41 (4)	0.053 (3)	234 (22)	646 (5)	216
Algiflor	0.00304 (5)	138 (11)	2.17 (2)	0.323 (2)	82 (20)	226 (3)	76
Cladophora	0.554 (1)	98.1 (6)	2.13 (2)	4.66 (5)	130 (6)	482 (2)	161

For capillaries with a diameter around 4-5 nm, the Kelvin equation predicts condensation of water at relative pressures x=0.60 (or 60% RH). This value coincides with the onset of stage three in the Zografi et al. (1984) model featuring the presence of bulk water. Bulk water would be expected to cover the entire surface of cellulose microfibrils, which would correspond to fractal dimensions D between 2 and 3. However, the D values obtained with H_2O mfBET were between 1 and 2, indicating site-specific interactions. Site-specific interactions are feasible only for the initial stages of the moisture sorption model proposed by Zografi et al. (1984) and not for stage three. Fractal theory could also be applied to account for the possibility of capillary condensation. To be able to use fractal capillary condensation theory, it was assumed that, when moisture is adsorbed onto the contact surfaces of cellulose crystallites, it might cause swelling and reveal a fractal pore structure where each of the crystallites has a fractal surface. Table 4 shows that the fractal dimension of the Cladophora sample obtained using the fractal capillary condensation method was similar to that obtained with N_2 mfBET. Because water does not induce new pore networks in the Cladophora cellulose, the detected pore structure is similar to that observed with N_2. The D_{cc} value ~2 shows that the pore walls of the Cladophora cellulose have low tortuousity. The D_{cc} value for the rest of the samples ranged between ~2.60 and 2.70 for the adsorption and desorption curves, respectively. Such high D values indicate that water is distributed in a highly tortuous pore network

induced by swelling of the cellulose. These results are in close agreement with the findings by Hatzikiriakos and Avramidis (1994) who reported the D values of wood surfaces, including the capillary condensation effects, in the range of 2.5 and 2.8.

Table 4. *Capillary condensation fractal dimensions of cellulose powders.*

	D_{cc} adsorption	D_{cc} desorption
LCC	2.70	2.73
AMC	2.61	2.67
MCC	2.69	2.66
Algiflor	2.60	2.57
Cladophora	2.17	2.19

Nicotine sorption by cellulose powders

The data for loading cellulose with nicotine are summarized in Table 5. The highest degree of sorption was found in the Cladophora cellulose sample and the lowest in the LCC sample. It was possible to incorporate much more nicotine via the rotary evaporation method than from nicotine-saturated air. The degree of nicotine sorption from nicotine-saturated air increased as the temperature was raised. The temperature-dependent pattern of sorption from nicotine-saturated air may have been due to a higher nicotine concentration in air at higher temperatures (Banyasz, 1999). However, no relationship between cellulose crystallinity index and degree of nicotine sorption was observed with either of the loading techniques. This implies that all the nicotine was distributed either in the voids between the cellulose particles (i.e. external pores) or in the open pores inside the particles (i.e. internal pores) but not in the bulk of the particles.

Table 5. *Nicotine loading by rotary evaporation and from nicotine-saturated air. The values in parentheses are standard deviations in percent (n=3).*

	Nicotine content, mg/g			
	By rotary evaporation	22°C*	40°C*	60°C*
LCC	164 (1.83)	1.5 (0.47)	2.0 (0.75)	3.2 (0.59)
AMC	190 (6.42)	2.3 (0.30)	3.6 (0.69)	4.9 (0.63)
MCC	193 (1.08)	1.9 (0.73)	3.4 (0.82)	4.4 (0.77)
Cladophora	453 (3.10)	33.2 (0.51)	109 (1.23)	196 (0.75)

*from nicotine-saturated air.

Given the lack of sorption in the bulk of the Cladophora cellulose particles and the pore volume values obtained from N_2 gas adsorption, it would theoretically be possible to accommodate up to 554 mg of nicotine per g of the

Cladophora powder (density of nicotine at 20°C is 1.0 g/cm^3), whereas the degree of sorption for the other samples should be around 4-5 mg of nicotine per gram. Indeed, the amount of nicotine incorporated into the cellulose from nicotine-saturated air was of the same order of magnitude as that predicted from N_2 gas adsorption. However, with rotary evaporation, it was possible to load about 160-190 mg of nicotine per gram of MCC, AMC, or LCC. This implies that, when loaded via rotary evaporation, nicotine is predominantly located in the voids. On the other hand, the degree of nicotine sorption for Cladophora cellulose when rotary evaporation was used did not exceed 554 mg/g; hence, it is likely that in this case nicotine is predominantly accommodated in the internal pores.

The pattern of nicotine release into an air-stream is shown in Figure 9 (on the left) as the decrease in the nicotine content of the cellulose powders (%, w/w) plotted against the volume of the passing air. Almost all the nicotine was released from the LCC sample. In the rest of the samples, the release was incomplete (about 20% remained in the Cladophora cellulose sample and about 50% in MCC and AMC). The incomplete release profile of nicotine from the cellulose powders could be attributed to various inclusion phenomena that have previously been observed in cellulose (Yiannos, 1965).

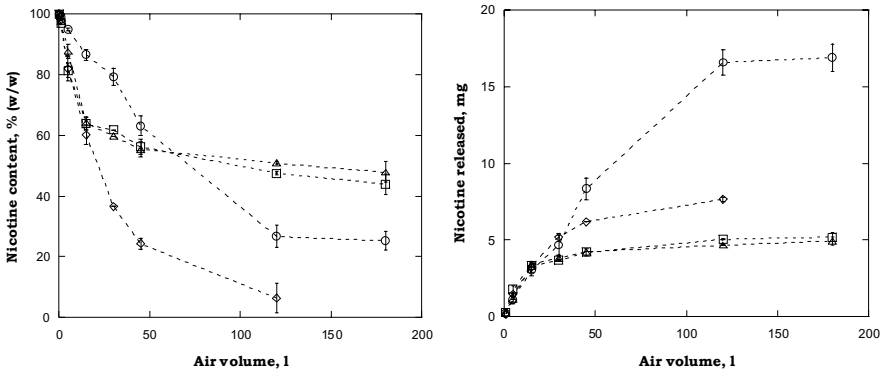

Figure 9. Release of nicotine into an air-stream. The decrease in nicotine content as a function of the passing air volume is shown on the left. The total amount of released nicotine against the air volume passing through a cellulose plug is shown on the right. The air-flow rate was 1.0 l/min. Lines are provided as guides for the eye. □ MCC, Δ AMC, ◊ LCC, and ○ Cladophora cellulose.

The right-hand graph in Figure 9 plots the total amount of released nicotine against the volume of passed air. The total amount of nicotine released from Cladophora cellulose powder was markedly higher than that from the other samples. Release of nicotine from the Cladophora sample occurred over an extended period of time, and a plateau region was achieved after 120 min (air-flow rate 1 l/min). However, this was not the case for the rest of the

samples, where the plateau region was reached after around 40-50 min. There was no apparent relationship between the release of nicotine into the air-stream and the cellulose crystallinity index.

The release of nicotine into water is summarized in Table 6. Most of the nicotine was released rapidly, within 5 min. It was released more rapidly and to a greater extent (~98%, w/w) from the Cladophora cellulose sample; the portion released from the MCC, AMC, and LCC samples was lower (~90-95%, w/w). As above, there was no apparent relationship between the release of nicotine into water and the cellulose crystallinity index. The almost immediate release into water is in accordance with an earlier report (Nasr et al., 1998).

Table 6. *Nicotine release into water. The values in parentheses are standard deviations in percent (n=3).*

	Nicotine released, % (w/w)		
	5 min	60 min	180 min
LCC	88.7 (6.30)	95.0 (8.50)	96.0 (7.39)
AMC	85.5 (2.69)	90.1 (0.89)	90.5 (1.40)
MCC	87.0 (5.10)	94.9 (5.39)	88.5 (8.13)
Cladophora	97.3 (6.06)	98.3 (2.03)	98.9 (4.15)

Because neither the loading extent nor the release profile were influenced by the cellulose crystallinity index, only Cladophora cellulose (a porous material) and MCC (a non-porous material) were investigated for stability. The nicotine content remained essentially intact in the Cladophora cellulose sample after 3 months of storage (recovery 101.7%, w/w) but there was a significant loss from MCC over the same time (recovery 60.2%, w/w). The concentration of nicotine-related degradation products after 3 months of storage, Table 7, was low in the Cladophora cellulose sample (0.90%, w/w), but substantial in the MCC sample (23.6%, w/w).

Table 7. *Nicotine degradation products formed during 3 months of storage.*

Degradation product	Concentration of degradation products, % (w/w)	
	Cladophora	MCC
Cotinine	0.30	2.82
Nicotine-*cis*-N-oxide	0.15	7.02
Nicotine-*trans*-N-oxide	0.29	11.4
MMP*	-	0.30
Myosmine	0.16	1.68
β-nicotyrine	-	0.36
Sum of degradation products	0.90	23.6

*MMP is methanone-(1-methyl-3-pyrrolydinyl)-3-pyridinil-; CAS 125630-26-4.

This difference could be interpreted in terms of exposure of nicotine to oxygen and the distribution of nicotine in the powder pore network: when nicotine is located in the internal pores, the amount of nicotine in direct contact with air is considerably lower than when nicotine is located in the voids. Hence, the highly porous matrices of the Cladophora cellulose particles would provide protection against the oxidative degradation of nicotine.

Solid-state stability of ASA in mixtures with cellulose

The ASA degradation patterns in physical mixtures and those prepared via rotary evaporation are presented in Figures 10 and 11. ASA was very stable in mixtures with LCC for both of the loading techniques. The degradation rates observed in the Cladophora sample were of the same order of magnitude for both of the loading techniques, whereas they were markedly different in the MCC and AMC samples. This was probably because ASA was partly located within the bulk of the MCC and AMC particles when loaded via rotary evaporation whereas, in the Cladophora sample, ASA was located exclusively on the walls of open pores, irrespective of the loading technique. It should be noted that LCC had a lower capacity than MCC or AMC to incorporate drugs as earlier observed with nicotine. The most dramatic differences between the loading techniques were observed for MCC/ASA and AMC/ASA mixtures at low and intermediate RHs: almost a ten-fold increase in the extent of degradation was observed when ASA was partly loaded into the bulk of the cellulose particles, where moisture sorption predominantly occurs.

It was also found that the influence of cellulose crystallinity index on ASA degradation was crucial only for a certain range of RHs. This is consistent with our findings that the moisture content of cellulose powders is strongly correlated with the crystallinity index at RHs below 75% whereas, at higher RHs, large surface area and pore volume take precedence in governing the moisture sorption pattern via capillary condensation.

High degradation rates observed in the Cladophora cellulose emphasize the importance of cellulose surface area (or pore volume). A similar effect was observed in dicalcium phosphate dihydrate (DCPD) powders by Landín et al. (1994) when higher rates of ASA degradation were observed as the surface area of DCPD was increased. Since the average pore diameter in the Cladophora sample was around 20 nm, the findings of this thesis are also in agreement with results reported by Yonemochi et al. (1991) who observed high degradation rates in controlled-pore glass bead mixtures with pore diameters below 30 nm.

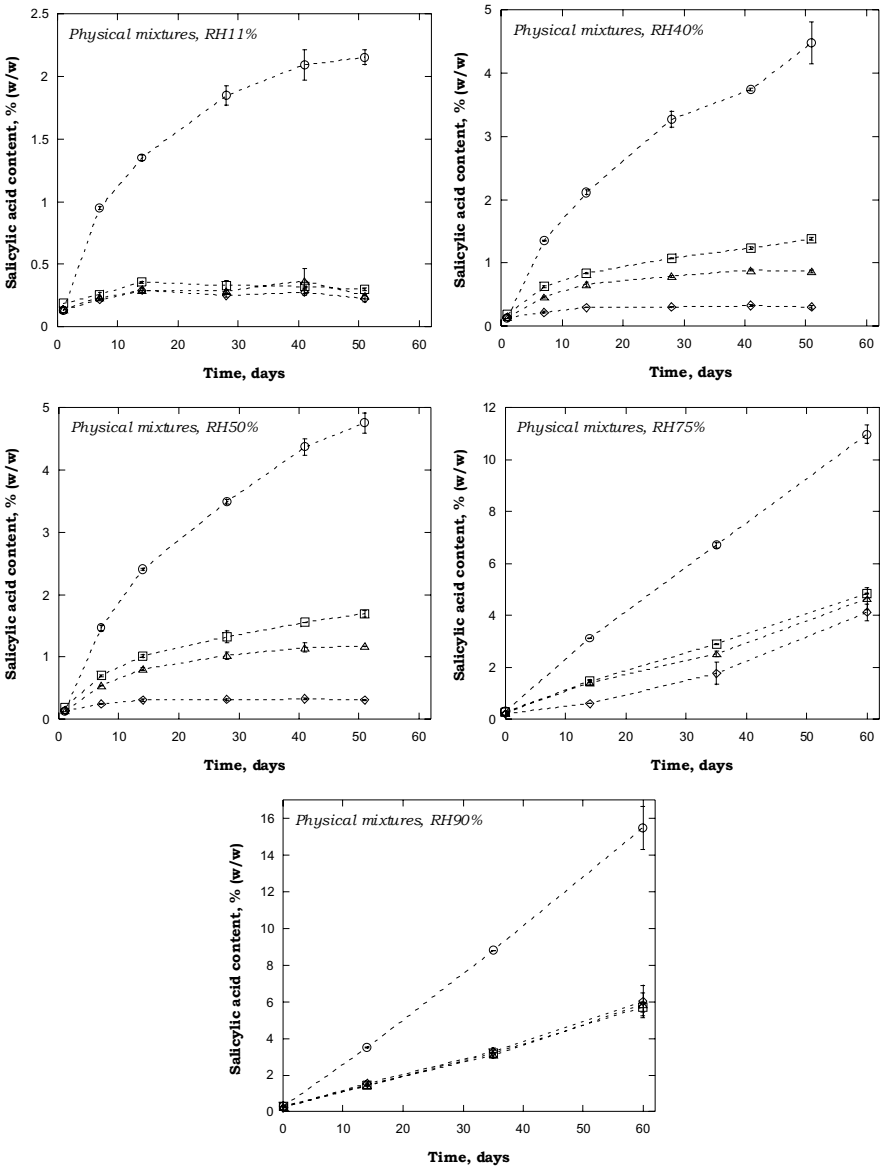

Figure 10. ASA degradation in physical mixtures. Lines are provided as guides for the eye. □ MCC, Δ AMC, ◊ LCC, and ○ Cladophora cellulose.

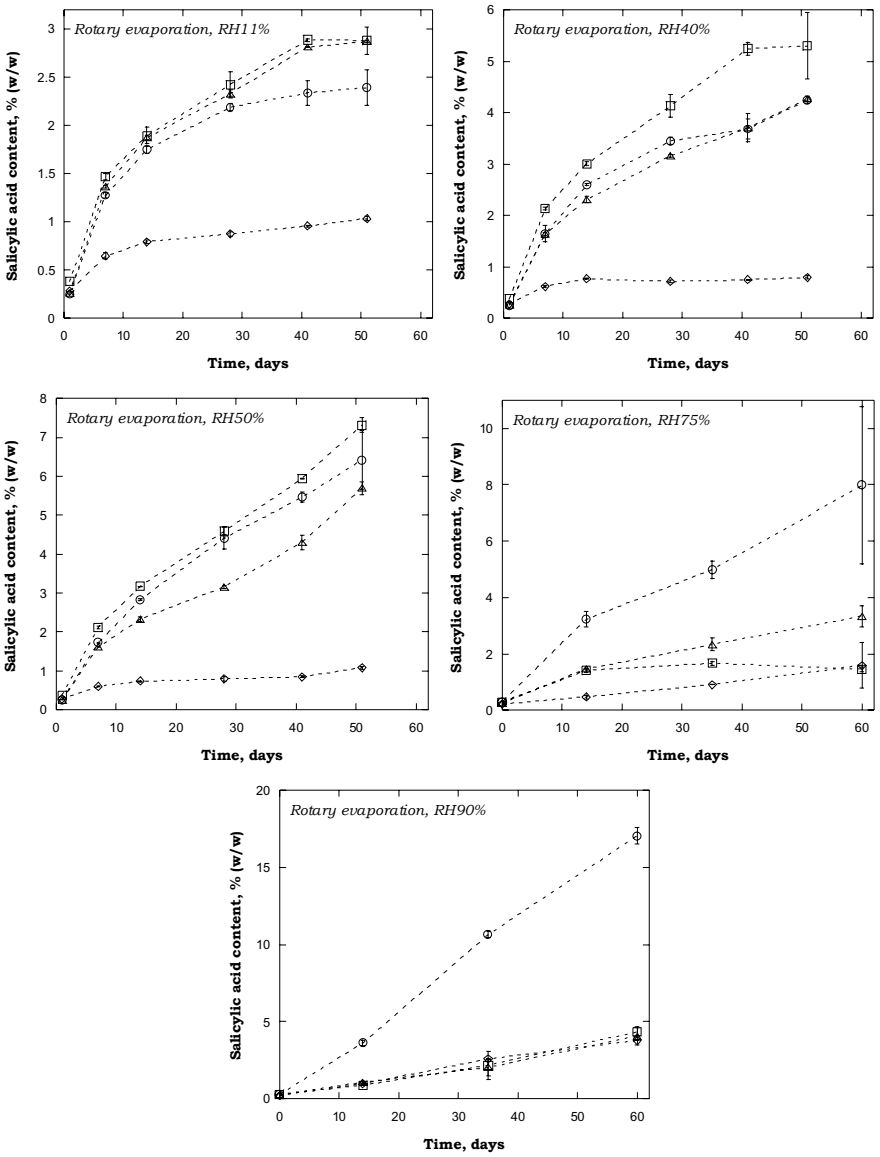

Figure 11. ASA degradation in mixtures loaded via rotary evaporation. Lines are provided as guides for the eye. □ MCC, Δ AMC, ◊ LCC, and ○ Cladophora cellulose.

The lower rates of degradation observed in the physical mixtures compared to those observed in the samples prepared via rotary evaporation highlight the importance of the availability of moisture in the induction of hydrolysis. One parameter that reflects the ability of cellulose to hold moisture is the hysteresis loop between the moisture adsorption and desorption curves. The

lower the crystallinity index of cellulose, the broader the hysteresis loop at low and intermediate RHs, Figure 8. Therefore, broad hysteresis loops at low RHs could be indicative of the material's ability to act as an internal dessicant. On the other hand, large hysteresis loops at high RHs are characteristic for porous substances and generally arise because of capillary condensation in open pores. Thus, large hysteresis loops at high RHs could be indicative of an increased propensity to facilitate undesired hydrolysis.

The degradation of ASA in cellulose powders, at least in this study, appeared not be governed by the nucleation-and-growth process because, for this class of solid-state reactions, S-shaped degradation curves are typically observed (Carstensen and Attarchi, 1988; Ball, 1994). Further, it appears that the degradation of ASA in mixtures with cellulose at high RHs is a pseudo-zero order process, typical of the degradation of substances in suspensions. This interpretation is in line with the Leeson-Mattocks theory of degradation in liquid films (Leeson and Mattocks, 1958). The degradation of ASA at low and intermediate RHs could theoretically be both diffusion-controlled and a second-order process. However, second-order kinetics would require the assumption of non-sink conditions (under the sink conditions the model reduces to the pseudo-first and pseudo-zero order kinetics). Further study is required to elucidate the true mechanism of degradation.

Summary and conclusions

The crystallinity index of the cellulose samples had a marked effect on the moisture sorption patterns at RHs below 75%, whereas the surface area and pore volume of the cellulose samples took precedence at higher RHs. It was also found that the hysteresis loops observed between the moisture adsorption and desorption curves of isotherms could have different origins at different RHs. This knowledge could give an insight into the distribution of moisture within the cellulose powder bed.

The theory of physical adsorption on fractal surfaces was found to be an alternative and powerful tool for describing moisture sorption phenomena occurring in the bulk of individual cellulose particles. It provided information about the inner nanoscale morphology of cellulose, which was not available using conventional methods, such as SEM, and also about the distribution of water within the cellulose.

An attempt was also made, using the above knowledge, to improve the pharmaceutical functionality of native cellulose powders in connection with the sorption of liquid drugs and moisture-related instability phenomena in the solid-state. There was no apparent relationship between the cellulose crystallinity index and the capacity of the samples to adsorb nicotine. On the other hand, the highly porous particles of the Cladophora cellulose powder not only exhibited a markedly high capacity to accommodate nicotine but also had a high capacity to prevent oxidative degradation of nicotine.

Whilst Cladophora cellulose powder was found useful for improving the stability of nicotine against oxidative degradation, the structure of the Cladophora cellulose particles also facilitated undesired hydrolytic degradation of ASA in the solid-state. This effect was attributed to a combination of both high crystallinity index and large surface area (and pore volume). The distribution of moisture between cellulose and ASA, as indicated by the presence of a hysteresis loop at various RHs, was suggested to be key for understanding ASA stability issues in mixtures with cellulose. Swelling MCC in 70 % (w/w) $ZnCl_2$ solution resulted in a product which enabled avoidance of ASA degradation as previously reported for commercial grades of MCC.

In all, this thesis demonstrates how the pharmaceutical functionality of MCC can be improved via engineering of the structure of native cellulose powders.

Acknowledgements

The work in this thesis was carried out at the Department of Pharmacy, Uppsala University, and partly at the former Pharmacia Consumer Healthcare, Helsingborg. The Swedish Institute (SI) and the Swedish Foundation for Strategic Research (SSF) are acknowledged for their financial support.

I would like to express my sincere gratitude to:

My supervisors, Associate Professor Ragnar Ek, for introducing me to the cellulose world and triggering in me the industry-oriented pattern of thinking, and Professor Maria Strømme, for her massive enthusiasm and always being there when I needed it most.

My co-authors, for their contributions to our work, and those who helped me in performing various experiments. Dr. Richard Karmhag and Nils Olov Ersson are commended with especial gratitude.

Professor Göran Alderborn, Head of the Department, for providing excellent research facilities and for many mind-provoking discussions. It has been an honor and privilege to be a part of "Galeniken".

Professor Per Artursson who kindly assisted me in coming to Sweden.

Staff at the Department of Pharmacy responsible for administrative, technical and IT support.

Dr. Nils-Olof Lindberg, a patent co-author, for his wise advice on various issues. Sven-Börje Andersson and Dr. Bengt Bosson, also co-authors, for motivating discussions. Staff at the former Pharmacia Consumer Healthcare, for taking good care of me and making me feel welcome during my stay in Helsingborg.

My office-mates, Dr. Jonas Berggren, for setting the standard of our office to the record heights (2.00m ± 4cm), and Christian Johansson, for increasing the entropy of my life. I could not have possibly had better "roomies".

All former and present fellow colleagues at the Department of Pharmacy, for keeping the working milieu joyful and motivating.

All former and present members of the powder and pharmaceutical materials science groups, for stimulating scientific discussions and much more: Dr. Johan Carlfors, Dr. Christina Gustafsson, Dr. Sofia Mattsson, Dr. Susanne Bredenberg, Dr. Jonas Berggren, Dr. Åsa Tunon, Dr. Sitaram Velaga, Dr. Denny Mahlin, Frauke Fichtner, Jessica Elversson, Josefina Hellström, Mina Heidarian, Ken Welch, Martin Nilsson, Ulrika Brohede, Nelly Fransén, and Per Nydert.

My dear friends with whom I have shared many different interests, experiences and plenty of mutual sympathy: Niclas Petri, Dr. Christer Tannergren, Carola Wassvik, Dr. Helene Hägerström, Dr. Björn Jansson, Dr. Jonas and Sofia Berggren, Dr. Linda Stertman, Christian Johansson, Dr. Christel Bergström, Dr. Denny Mahlin, Elin Sjödin, and, of course, Lucia Lazorova as well as the Italo-Catalan "Foreign Legion": Assum Piñas Llagostera, Francesca Caprani, Gemma Feliu, and Andrea Meinero.

Johan "Giovanni" Wetterberg (aka "The Admiral") and Per Nydert, for extracurricular activities.

Andreas Månsson and the other Erasmus comrades from Sweden, Spain, Italy, Germany, and Belgium, for their encouragement and all the fun we had when paying mutual visits.

Dr. Arman Zakaryan, for sharing the "hardships" of my first year in Sweden. Tsolak Sargsyan, Vigen Voskanyan, and David Gevorgyan, for their friendship despite the long distance between us.

My relatives, for being helpful in so many different ways and on so many different levels. Uncle Leonid without whom I would never become a pharmacist in the first place, aunt Nina, for her solid support, and aunt Nara, for her infinite kindness. Special thanks to aunt Alvina and uncle-in-law Aris!

My parents, for all the sacrifices they made to make my dreams come true, and, more importantly, for raising me a person with a free and open mind.

References

Ahlneck, C., Lundgren, P. (1985). "Methods for the Evaluation of Solid-State Stability and Compatibility between Drug and Excipient." Acta Pharm Suec 22(6): 305-314.

Ahlneck, C., Alderborn, G. (1988). "Solid state stability of acetylsalicylic acid in binary mixtures with microcrystalline and microfine cellulose." Acta Pharm Suec 25(1): 41-52.

Alderborn, G., Nyström, C. (1993). Characterization of powder surface areas. Industrial aspects of pharmaceutics. Sundell, E. (Ed.). Stockholm, Swedish Pharmaceutical Press: 7-22.

Anderson, R. B. (1946). "Modifications of the Brunauer, Emmett and Teller equation." J Am Chem Soc 68: 686-691.

Astbury, W. T. (1945). "Structure of Alginic acid." Nature 155: 667-668.

Avnir, D., Pfeifer, P. (1983). "Fractal dimension in chemistry. An intensive characteristic of surface irregularity." Nouv J Chim 7: 71-72.

Avnir, D., Jaroniec, M. (1989). "An isotherm equation for adsorption on fractal surfaces of heterogeneous porous materials." Langmuir 5(6): 1431-1433.

Avnir, D., Farin, D., Pfeifer, P. (1992). "A discussion of some aspects of surface fractality and of its determination." New J Chem 16(4): 439-449.

Ball, M. C. (1994). "Solid-State Hydrolysis of Aspirin." J Chem Soc Faraday Trans 90(7): 997-1001.

Banyasz, J. L. (1999). The physical chemistry of nicotine. Analytical determination of nicotine and related compounds and their metabolites. Gorrod, J. W., Peyton III, J. (Eds.). Amsterdam, Elsevier: p. 154.

Bear, R. S. (1944). "X-ray diffraction studies on protein fibers. I. The large fiber-axis period of collagen." J Am Chem Soc 66: 1297-1305.

Blair, T. C., Buckton, G., Beezer, A. E., Bloomfield, S. F. (1990). "The interaction of various types of microcrystalline cellulose and starch with water." Int J Pharm 63(3): 251-257.

Brady, R. M., Ball, R.C. (1984). "Fractal growth of copper electrodeposits." Nature 309: 225-229.

Brunauer, B., Emmett, P.H., Teller, E. (1938). "Adsorption of gases in multimolecular layers." J Am Chem Soc 60: 309-319.

Carstensen, J. T., Attarchi, F. (1988). "Decomposition of Aspirin in the Solid-State in the Presence of Limited Amounts of Moisture. 3. Effect of Temperature and a Possible Mechanism." J Pharm Sci 77(4): 318-321.

Cohan, L. H. (1938). "Sorption hysteresis and the vapor pressure of concave surfaces." J Am Chem Soc 60: 433-435.

de Boer, J. H. (1968). The dynamical character of adsorption, 2nd ed. Oxford, Clarendon Press.

Doelker, E., Gurny, R., Schurz, J., Janosi, A., Matin, N. (1987). "Degrees of crystallinity and polymerization of modified cellulose powders for direct tableting." Powder Tech 52(3): 207-213.

Ek, R., Wormald, P., Ostelius, J., Iversen, T., Nyström, C. (1995). "Crystallinity index of microcrystalline cellulose particles compressed into tablets." Int J Pharm 125(2): 257-264.

Ek, R., Gustafsson, C., Nutt, A., Iversen, T., Nyström, C. (1998). "Cellulose powder from Cladophora sp. algae." J Mol Recognit 11(1-6): 263-265.

Encyclopaedia Britannica. (2003). Dynamite, Encyclopaedia Britanica Online. 2003.

European Pahrmacopoeia, 4th edn. (2002). Strasbourg, Council of Europe.

Flory, P. J. (1953). Principles of polymer chemistry. Ithaca, New York, Cornwell University Press.

Guggenheim, E. A. (1966). Applications to statistical mechanics. Oxford, Clarendon Press.

Gustafsson, C., Lennholm, H., Iversen, T., Nyström, C. (2003). "Evaluation of surface and bulk characteristics of cellulose I powders in relation to compaction behavior and tablet properties." Drug Dev Ind Pharm 29(10): 1095-1107.

Hailwood, A. J., Horrobin, S. (1946). Absorption of water by polymers: Analysis in terms of a simple model. Trans Farad Soc 42B: 84-92.

Hancock, B. C., Zografi G. (1993). "The use of solution theories for predicting water vapor absorption by amorphous pharmaceutical solids: a test of the Flory-Huggins and Vrentas models." Pharm Res 10(9): 1262-1267.

Handbook of pharmaceutical excipients, 2nd edn. (1994). London, Pharmaceutical Press.

Hatzikiriakos, S. G., Avramidis, S. (1994). "Fractal Dimension of Wood Surfaces from Sorption Isotherms." Wood Sci Techn 28(4): 275-284.

Hill, T. L. (1946). "Statistical mechanics of multimolecular adsorption." J Chem Phys 14(4): 263-267.

Hill, T. L. (1952). "Theory of physical adsorption." Adv Cat 4: 211-258.

Hollenbeck, R. G., Peck, G. E., Kildsig, D. O. (1978). "Application of immersional calorimetry to investigation of solid-liquid interactions: microcrystalline cellulose-water system." J Pharm Sci 67(11): 1599-1606.

Horii, F., Hirai, A., Kitamaru, R. (1987). "CP/MAS C-13 NMR-spectra of the crystalline components of native celluloses." Macromolecules 20(9): 2117-2120.

Howsman, J. A. (1949). "Water sorption and the poly-phase structure of cellulose fibers." Textile Res J 19: 152-162.

Hulbert, S. F. (1970). "Models for solid-state reactions in powdered compacts: A review." Brit Cer Soc 1: 11-20.

Jackson, K. E. (1941). "Alkaloids of tobacco." Chem Rev 29: 123-197.

Kelvin, J. (published under the name of Sir William Thomson). (1871). Phil Mag 42: 448-452.

Landín, M., Perezmarcos, B., Casalderrey, M., Martinez-Pacheco, R., Gomez-Amoza, J. L., Souto, C., Concheiro, A., Rowe, R. C. (1994). "Chemi-

cal-Stability of Acetylsalicylic-Acid in Tablets Prepared with Different Commercial Brands of Dicalcium Phosphate Dihydrate." Int J Pharm 107(3): 247-249.

Leeson, L. J., Mattocks, A. M. (1958). "Decomposition of aspirin in the solid state." J Am Pharm Assoc Am Pharm Assoc (Baltim) 47(5): 329-333.

Leuenberger, H., Leu, R., Bonny, J.D. (1996). Application of percolation theory and fractal geometry to tablet compaction. Pharmaceutical powder compaction technology. Alderborn, G., Nyström, C. (Eds.), New York, Marcel Dekker: 133-164.

Mandelbrot, B. B. (1982). The fractal geometry of nature. San Francisco, CA, Freeman.

Marchessault, R. H., Sarko, A. (1967). X-ray structure of polysaccharides. Advanced carbohydrate chemistry. Wolform, M. L. (Ed.). New York, Academic press: 421-483.

Marchessault, R. H., Sundararajan, P.R. (1983). Cellulose. The polysaccharides. Aspinall, G. (Ed.). New York, Academic Press. 2: p. 11.

Nakai, Y., Fukuoka, E., Nakajima, S., Hasegawa, J. (1977). "Crystallinity and physical characteristics of microcrystalline cellulose." Chem Pharm Bull 25: 96-101.

Nelson, M. L., O'Connor, R.T. (1964). "Relation of certain infrared bands to cellulose crystallinity and crystal lattice type. Part I. Spectra of lattice types I, II, III and of amorphous cellulose. Part II. A new infrared ratio for estimation of crystallinity in cellulose I and II." J Appl Pol Sci 8: 1311-1341.

Nyqvist, H. (1983). "Saturated salt solutions for maintaining specified relative humidities." Int J Pharm Tech Prod Mfr 4: 47-48.

Nasr, M. M., Reepmeyer, J. C., Tang, Y. (1998). In vitro study of nicotine release from smokeless tobacco, J AOAC Int 81: 540–543.

O'Sullivan, A. (1997). "Cellulose: the structure slowly unravels." Cellulose 4(3): 173-207.

Patil, N. B., Dweltz, N.E., Radhakrishnan, T. (1965). "Studies on decrystallization of cotton." Textile Res J 35: 517-523.

Payen, A. (1838). "Memoire sur la composition du tissu proper des plantes et du ligneux." Comptes Rendus 7: 1052-1056.

Pfeifer, P., Avnir, D. (1983). "Chemistry of noninteger dimensions between two and three. I. Fractal theory of heterogeneous surfaces." J Chem Phys 79(7): 3558-3565.

Pfeifer, P., Obert, M., Cole, M.W. (1989a). "Fractal BET and FHH theories of adsorption: a comparative study." Proc R Soc Lond A 423: 169-188.

Pfeifer, P., Wu, Y. J., Cole, M. W., Krim, J. (1989b). "Multilayer adsorption on a fractally rough-surface." Phys Rev Letters 62(17): 1997-2000.

Pfeifer, P., Ehrburger-Dolle, F., Rieker, T.P., Gonzalez, M.T., Hoffman, W.P., Molina-Sabio, M., Rodriguez-Reinoso, F., Schmidt, P.W., Voss, D.J. (2002). "Nearly space-filling fractal networks of carbon nanopores." Phys Rev Letters 88(11): 115502(4).

Pomonis, P. J., Ladavos, A.K. (2002). Adsorption of gases at porous solid surfaces. Encyclopedia of Surface and Colloid Science, Marcel Dekker: 354 - 372.

Rouquerol, J., Avnir, D., Fairbridge, C. W., Everett, D. H., Haynes, J. H., Pernicone, N., Ramsay, J. D. F., Sing, K. S. W., Unger, K. K. (1994). "Recommendations for the characterization of porous solids." Pure Appl Chem 66(8): 1739-1758.

Russel, M. A. H. (1988). "Nicotine replacement: The role of blood nicotine levels, their rate of change, and nicotine tolerance." Prog Clin Biol Res 261: 63-94.

Schaefer, D. W., Keefer, K. D. (1986). "Structure of random porous materials: Silica aerogel." Phys Rev Letters 56(20): 2199-2202.

Segal, L., Creely, J.J., Martin Jr, A.E., Conrad, C.M. (1959). "An empirical method of estimating the degree of crystallinity of native cellulose using the X-ray diffractometer." Textile Res J 29: 786-794.

Šeštak, J., Šatava, V., Wendlandt, W.W. (1973). "The study of heterogeneous processes by thermal analysis." Thermochim Acta 7(5): 333-556.

Sing, K. S. W., Everett, D.H., Haul, R.A.W., Moscou, L., Pierotti, R.A., Rouquerol, J., Siemienewska, T. (1985). "Reporting physisorption data for

gas/solid systems with special reference to the determination of surface area and porosity (recommendations)." Pure Appl Chem 57: 603-619.

Sjöstrom, E. (1981). Wood chemistry fundamentals and application. New York, Academic Press.

Ståhlberg, J. (1991). Functional organisation of cellulose from Trichoderma reesei, PhD thesis, Uppsala University.

Stubberud, L., Arwidsson, H. G., Larsson, A., Graffner, C. (1996). "Water solid interactions. 2. Effect of moisture sorption and glass transition temperature on compactibility of microcrystalline cellulose alone or in binary mixtures with polyvinyl pyrrolidone." Int J Pharm 134(1-2): 79-88.

Suzuki, T., Nakagami, H. (1999). "Effect of crystallinity of microcrystalline cellulose on the compactability and dissolution of tablets." Eur J Pharm Biopharm 47(3): 225-230.

Svensson, C. K. (1987). "Clinical Pharmacokinetics of Nicotine." Clin Pharmacokinet 12(1): 30-40.

Valentine, L. (1958). "Studies on the sorption of moisture by polymers. I. Effect of crystallinity." J Polymer Sci 27(115): 313-333.

vander Hart, D. L., Atalla, R.H. (1984). "Studies of macromolecules in native cellulose using solid-state 13C NMR." Macromolecules 17: 1465-1472.

Verlhac, C., Dedier, J., Chanzy, H. (1990). "Availability of surface hydroxyl-groups in Valonia and bacterial cellulose." J Polymer Sci Part A-Polymer Chem 28(5): 1171-1177.

Vrentas, J. S., Vrentas, C. M. (1994a). "Solvent self-diffusion in glassy polymer-solvent systems." Macromolecules 27(20): 5570-5576.

Vrentas, J. S., Vrentas, C. M. (1994b). "Solvent self-diffusion in rubbery polymer-solvent systems." Macromolecules 27(17): 4684-4690.

Walton, A. G., Blackwell, J. (1973). Biopolymers. New York, Academic Press. 22: p. 468.

Wickholm, K., Larsson, P.T., Iversen, T. (1998). "Assignment of non-crystalline forms in cellulose I by CP/MAS 13C-NMR spectroscopy." Carbohydrate Res 312: 123-129.

Yiannos, P. N. (1965). Swellability of pulps determined by isopropanol retention, Tappi 48: 494–496.

Yin, Y. (1991). "Adsorption isotherm on fractally porous materials." Langmuir 7: 216-217.

Yonemochi, E., Matsumura, M., Oguchi, T., Yamamoto, K., Nakai, Y. (1991). "Interactions of Medicinals and Porous Powder - Stability of Aspirin in Controlled Pore Glass Solid Dispersions." Chem Pharm Bull 39(4): 1027-1031.

Zhang, J., Zografi, G. (2000). "The relationship between "BET" and "Free-volume-derived parameters for water vapor absorption into amorphous solids." J Pharm Sci 89(8): 1063-1072.

Zografi, G., Kontny, M.J., Yang, A.Y.S., Brenner, G.S. (1984). "Surface area and vapor sorption of microcrystalline cellulose." Int J Pharm 18: 99-116.

Zografi, G., Kontny M. J. (1986). "The interactions of water with cellulose-derived and starch-derived pharmaceutical excipients." Pharm Res 3(4): 187-194.

Acta Universitatis Upsaliensis

Digital Comprehensive Summaries of Uppsala Dissertations from the Faculty of Pharmacy 1

Editor: The Dean of the Faculty of Pharmacy

A doctoral dissertation from the Faculty of Pharmacy, Uppsala University, is usually a summary of a number of papers. A few copies of the complete dissertation are kept at major Swedish research libraries, while the summary alone is distributed internationally through the series Digital Comprehensive Summaries of Uppsala Dissertations from the Faculty of Pharmacy. (Prior to January, 2005, the series was published under the title "Comprehensive Summaries of Uppsala Dissertations from the Faculty of Pharmacy".)

Distribution: publications.uu.se
urn:nbn:se:uu:diva-4752

ACTA
UNIVERSITATIS
UPSALIENSIS
UPPSALA
2005